Multistage Friction Connection Optimisaton

G. A. MacRae

University of Canterbury, Christchurch, New Zealand

R. C. A. Brosnan

Fulton Hogan, Wellington, New Zealand

B. A. A. El-Mashalgi

GHD, Christchurch, New Zealand

Z. Luo

Xi'an University of Architecture and Technology, Xi'an, China

J. C. Chanchi Golondrino

Universidad Nacional de Colombia, Manizales - Caldas, Colombia

ABSTRACT

This paper describes the concept, construction, and optimisation of a multistage friction connection (MFC). For a MFC, push-pull analyses are conducted to validate the behaviour. Then, the MFC is incorporated in a simple single degree of freedom (SDOF) structure. Inelastic dynamic time history analysis (THA) is conducted to determine (i) the optimal ratio of the first sliding resistance to the second sliding resistance, and (ii) the optimal length of the first sliding stage, in order to minimise peak and residual displacements with and without considering the *P*-delta effect.

The MFC axial force resisting device comprises a symmetric friction connection (SFC) at each end. Each symmetric friction connection is assembled with a central slotted plate. The two central slotted plates are clamped to two external plates by means of pre-tensioned high strength bolts. In between the external plates and the slotted plates, high hardness shims are inserted. In the MFC energy is dissipated when the slotted plates slide in series. Fewer high strength bolts are placed at the MFC end which initially slides. Sliding stops at this end when bolts contact the ends of the slotted holes and bear on the plate. Sliding then occurs at a greater force at the other end of the MFC. Push-pull analyses demonstrated the expected performance, which was consistent with that from experimental testing. For a structure designed with a lateral force reduction factor of 4, bolt holes permitting an initial sliding distance in the direction of force corresponding to about 0.60 of the system's elastic displacement, and an initial sliding strength of about 0.4 times the final sliding strength, was optimal and resulting in the lowest peak and residual displacements for the cases considered.

INTRODUCTION

Many modern buildings are now designed so that they not only protect life, but also remain usable after a major earthquake. Such low damage, or resilience, concepts are accomplished by designing the structure to be very stiff or by equipping the structure with a seismic dissipaters. One easy-to-assemble, and cheap seismic dissipater, with very stable hysteretic behaviour is the symmetric friction connection (SFC). SFCs are characterized by fat hysteresis loops with very low post-elastic stiffness (Chanchi Golondrino et al., 2023). While inelastic deformation may be concentrated in these structures, thereby protecting other elements of the building skeleton from earthquake effects, the structure may have large cumulative inelastic displacements in one direction, especially when P-delta effects also contribute to the response. Such phenomena is referred to as seismic ratcheting. This may result in large post-shaking residual displacements or the structure, or even collapse.

One way to mitigate the possibility of seismic ratcheting, without increasing the strength, is to change the hysteresis loop of the structure so that it tends to be more pinched. For this to be practical, the process of making a pinched loop should not be excessively expensive, and the hysteresis loop itself should be such that it effectively reduces seismic peak and residual displacements.

The multistage friction connection (MFC) concept has been recently proposed (MacRae, 2021). Initial testing showed the MFC hysteresis loop has two stages with different strengths (Chanchi Golondrino et al., 2023). Such a hysteretic loop is pinched, and it may be desirable to mitigate seismic ratcheting. However, the effectiveness of MFCs in a structure to mitigate ratcheting has not been investigated. Also, the effects of the possible range of strength ratio between the first and second sliding stages, and the range of sliding displacement that can occur in the first stage, has not been quantified.

For engineers considering designing structures equipped with MFCs, need to know (i) that MFCs can indeed reduce the response, and (ii) the design parameters that give the smallest structural demands. For this reason, this paper seeks answers to following questions:

1. What is a MFC, and how does it dissipates seismic energy?
2. Can a MFC be modelled?
3. Can the strength and sliding parameters be optimised to minimise peak and residual displacements?

1. PREVIOUS WORK

1.1 Seismic Ratcheting and Dynamic Stability

Seismic ratcheting refers to the phenomena by which structures predominately deform more in one direction compared to the other during an earthquake event. It can result in unexpected deformations, damage, or possible structural collapse. Ratcheting can occur due to a number of reasons (Saif et al., 2020; MacRae et al., 2023a; Baloch et al., 2024). One of the factors that can be controlled in design is the shape of the structural force-displacement hysteresis loop and this effect is not generally considered in routine seismic design. Structures with “dynamically unstable” hysteresis loops are most likely to experience ratcheting.

The dynamic stability of a hysteresis loop may be described below. Many structures, including those containing moment-resisting frames (MRF) and buckling restrained braced frames (BRBF) produce bilinear hysteresis loops when subject to cyclic lateral loading. If these structures have a positive post-elastic stiffness, such as those in Figure 1a, then ratcheting is unlikely. Consider a structure which is oscillating about point A in Figure 1a. Given that it is likely to have similar oscillations in both positive and negative force directions, it is more likely to yield at the lower yield line towards the initial displacement ($\Delta = 0$) position. Furthermore, if it reaches the peak force H_{yt} at its peak displacement during a response cycle, the velocity at that point is likely to be

zero. When it starts to move down the unloading curve, it will not just stop at point A, because it will have built up velocity as it unloads. Given the high velocity at point A, it will tend to continue down the curve and yield in the negative direction at point H_{yb}. Such as structure is considered dynamically stable (MacRae, 1994; MacRae and Kawashima, 1991; 1993; 1997; MacRae et al., 2023a). Conversely, if a structure has a negative post-elastic stiffness due to material, member local geometric effects such as buckling, or overall member geometric effects such as *P*-delta (or more correctly "*P*-theta", (Dehghanian et al. 2024)), then it is characterised as being dynamically unstable. Here, it may be seen that for an oscillator shaking about point A, yielding will tend to occur upper yield line at H_{yt} because it is closer to the zero force line. This causes the structure to yield away from the initial displacement location. During many loading cycles it could cause cumulative yielding in one direction. This seismic ratcheting is undesirable. The hysteresis centre curve (HCC) concept allows the degree of dynamic stability to be quantified. The HCC is the vertical centre point between the upper and lower yield limits of elastic response lines (MacRae 1994). For example, for the elastic response lines passing through point A in **Error! Reference source not found.**, a point on the HCC is found on that line as (H_{yt}+ H_{yb})/2. It can be found for all other elastic response lines to obtain the full HCC. When the HCC is in the 1st and 3rd quadrants, the structure is dynamically stable.

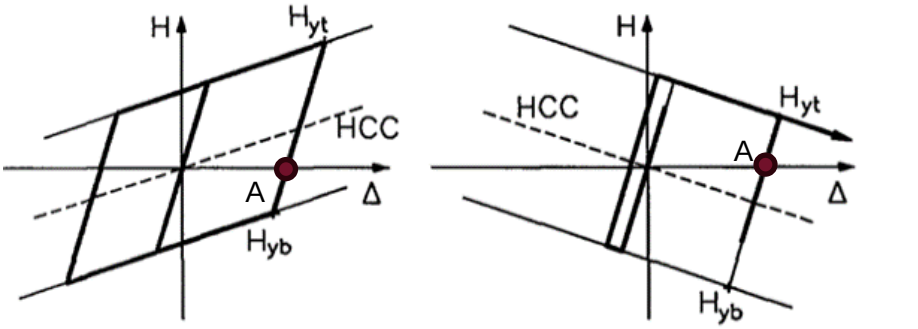

(a) Dynamically Stable *(b) Dynamically Unstable (P-delta)*

Figure 1. Dynamic stability concepts (MacRae 1994).

A couple of examples of structures found to have significant ratcheting due to structural hysteresis loop effects (considering also P-delta) are: (i) Steel bridge columns tested on the shaking table (MacRae and Kawashima, 1997; 2001), and (ii) BRB structures subjected to long duration earthquake ground motions where collapse occurred in the analyses conducted (Hariri and Tremblay 2019).

Some methods that may improve the performance of structures which may otherwise have a tendency to ratchet due to hysteresis loops with dynamic instability (MacRae, 2023, MacRae et al, 2023b) include:

a) Making a structure stronger so that it has a lower lateral force reduction factor, so the extend of yielding is limited. If it is strong enough, it will behave elastically with no ratcheting.

b) Making a structure stiffer, so that even if ratchetting does occur, displacements are likely to be small.

c) Using energy dissipation devices with self-centring tendencies. These include the self--centring brace (Christopoulos et al. 2008), the self-centring sliding hinge joint (Khoo et al. 2012), and many others.

d) Using devices which instead of increasing their strength to a certain stiffness, and remaining at that strength with little or no post-elastic stiffness, increase the strength in stages. These include (i) multistage buckling restrained braces (e.g. Sitler and Takeuchi 2020, 2021), steel dissipators (Li et al, 2022), and friction devices (Chanchi et al., 2023; 2024). It is noted that Chinese researchers have generally selected multistage devices, primarily considering yielding, in order to provide different levels or resistance at the serviceability and ultimate limit states rather than for considerations about dynamic stability.

e) Considering the effects of continuous columns (or walls, spines, stiffbacks, or strongbacks) within the structure to mitigate the possibility of dynamic instability over a few stories of the structure (MacRae et al. 2004, MacRae 2011).

f) Modifying the frame configuration to increase the dynamic stability (e.g. Tremblay and Darwiche, 2023).

g) Using different overall structural forms, such as rocking systems, base isolation etc.

h) Utilizing the effects of the building non-skeletal elements, such as the internal partition walls, and cladding (including precast concrete panels, and glazed curtain walls) which are designed to rock. E.g. Robertson et al. (2024).

1.2 Multistage Friction Connections

The behaviour of multistage friction connections (MFCs) to increase dynamic stability are described below. Some of these have been tested by Chanchí Golondrino et al. (2023, 2024). Figure 2a shows two central plates in green termed slotted plates because they have slotted holes. The yellow plates shown are high hardness shims with Brinell hardness of 500. These are located beside the fixed plates which have standard bolt holes. The two external plates in blue are termed fixed plates and they have standard bolt holes. The slotted plates and the fixed plates are made of Grade 300 steel or A36 steel. High strength bolts such as Grade 8.8 or A325 pass through the assembly of 5 plates/shims providing a clamping force. Washers, are generally placed below the head and nut of the bolts. The high strength bolts are tensioned to the proof load by the nut rotation method or by the calibrated torque control method.

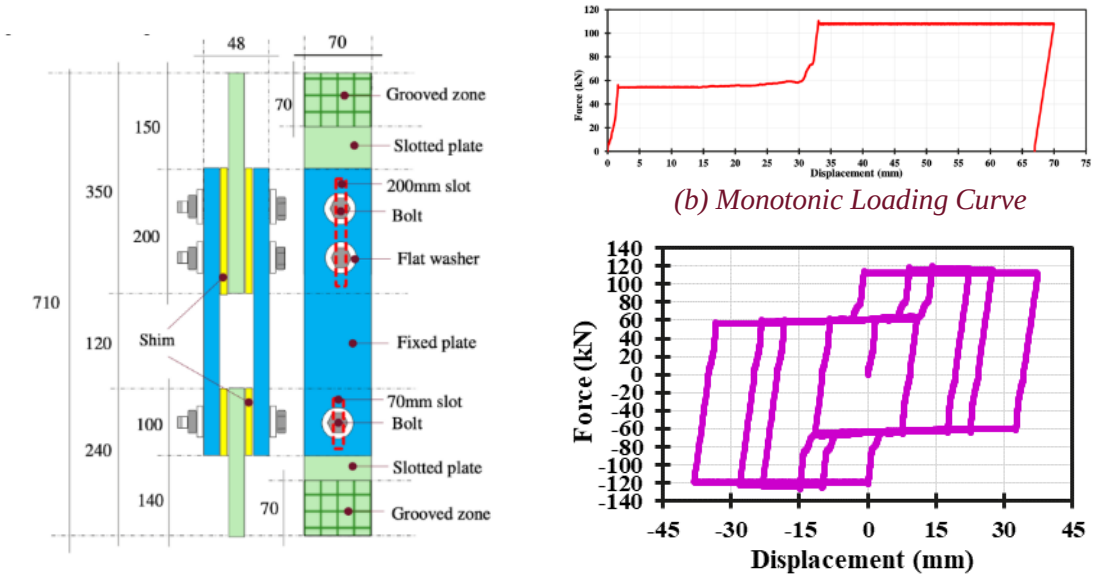

(a) Components *(b) Monotonic Loading Curve* *(c) Cyclic Curve*

Figure 1. *Two stage multistage friction connection (MFC) (Chanchí Golondrino et al. 2023, 2024).*

When axial tension/compression force is applied to the ends of the green plates, the MFC initially carries force elastically with no sliding, thus no inelastic dissipation occurs. When the frictional sliding force at the lower part of the MFC is reached, sliding occurs. The strength of this first stage of sliding occurs because there is only one bolt placed there providing a relatively small sliding force compared to the other end of the MFC. Sliding continues until the bolt shank reaches the edge of the slotted hole, and the force is then increased there due to bearing forces developed between the bolt shank and the slotted hole edge. The length of the first stage of sliding is therefore sensitive to the length of the slotted hole on the side of the device with the fewest bolts. The weakest part of the MFC now becomes the top connection which starts sliding at a force which should be approximately twice that in the first stage because there are twice as many bolts here and the bolts are tightened equally. It may be seen in Figure 2b that the first stage sliding occurs at about 55kN, while the second stage occurs at about 110kN indicating that the connection works as expected. Figure 2c shows the cyclic performance. It may be seen that this hysteretic loop shape is pinched, providing dynamic stability. The dynamic performance is dependent on both the relative strength ratios and the slot length. While a two stage

MFC is shown here, it is possible, by using more elaborate configurations to obtain many more friction stages, but this is not discussed further in this paper.

2 MODELLING

The simple linear model in Figure 3 was developed to represent the behaviour of a structure containing a MFC. In the model, the combined element between nodes N1 and N2 has a 'FC-1' component, a tension gap component, and a compression gap component. The element between N2 and N3 represents the second sliding stage of the MFC with the 'FC-2' component. The elastic stiffnesses of components 'FC-1', and 'FC-2' represent the steel material elastic behaviour of the slotted plates and fixed plates. The strengths of these components represents the connection sliding friction. In OpenSEES, the material code 'Steel01' was used. The tension and compression gap lengths represent the distance the that sliding can occur. The sum of these gap lengths is the total slot length minus the bolt diameter. These gap components were modelled using the element 'ElasticPPGap'. The 'ZeroLength' element was used. No tension gap or compression gap on the second element, representing the longer hole, was used. Node N1 was fixed, and nodes 2 and 3 were only permitted to move in the axial (x) direction.

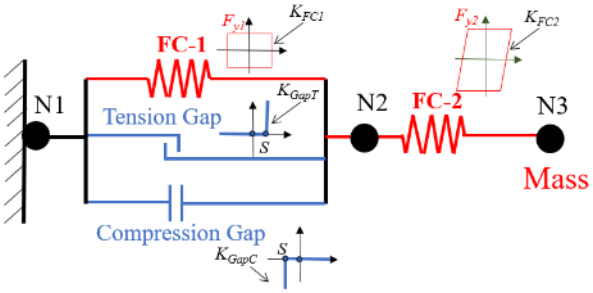

Figure 3. *MFC model.*

A benchmark model was developed. Tension and compression gap elements were made stiff and strong. The stiffnesses, E_o, were both 2,000,000 N/mm, and yield strengths, F_y, were 2 MN and – 2MN respectively. For components FC-1 and FC-2 the stiffnesses, E_o, were 1,000,000 N/mm, and 1,000 N/mm respectively, yield strengths, F_y, were 1,000 N, and 2,000N respectively, and the post-elastic stiffness ratios were 10^{-8} (which is very close to zero) for both in the non-P-delta case. The stiffness selection means that the initial stiffness of the structure was governed by the lower stiffness of FC-2. To give an indication of the structural behaviour with a loop with a negative post-elastic stiffness, such as when P-delta acts, the post-elastic stiffness ratios were changed to -0.00003 and -0.03 for FC-1 and FC-2 respectively. It is noted that the provide a better indication of the P-delta effect, the MFC model in Figure 3 could have been connected to a vertical pin-pin column element and a vertical gravity force, P, applied to the pin. In such a case, all stiffnesses would be reduced by P/L, where L is the column height.

The strength ratio, β, was defined as the ratio of the strength of the first sliding stage, F_{y1}/F_{y2}, as per Figure 3 and Equation 1. It is always less than or equal to unity.

$$\beta = F_{y1}/F_{y2} \quad (1)$$

For push-pull analysis, β = 0.5 was chosen with gaps of 0mm, 6mm and 15mm. Analysis was completed using displacement control with displacement increments of 0.1 mm.

For inelastic dynamic time history analysis, the structure was determined to have a fundamental natural period, T, of 1.0s, and the desired lateral force reduction factor, R, selected was 4.0. Since the stiffness of the structure, k, was already specified from the benchmark parameters above, the mass, m, placed at node N3 was determined as $m = k.(T/(2\pi))^2$ which was 25,310 kg.

The earthquake records that were chosen to perform the THA were the 22 pairs (44 records in total) of far-field earthquake records recommended by FEMA P695 (Fiorino et al. 2017). Zeros were added to the end of each earthquake record until the length of each record was at least 25 seconds longer than when the last acceleration became less than 1% of the peak acceleration. This allowed sufficient time for the free vibration so that the structure could settle down so that any residual/permanent displacement could be obtained.

The accelerations of all earthquake records were all initially scaled to provide the same spectral acceleration at the period of 1.0s (i.e. $S_{a,Target}(T=1.0s)$). The $S_{a,Target}(T=1.0s)$ value selected was $0.772g$. It is associated with the New Zealand earthquake loadings standard (NZS1170.5, 2004) for a normal importance level building (i.e. IL = 1.0) in Wellington on a site of Soil Class D considering an annual probability of exceedance, APE, of 1/500 years, and a near-fault factor, N, of 1.0.

The elastic force expected, F_e, was then calculated as $m.S_{a,Target}(T=1.0s)$ which is 191,681 N. the elastic displacement, Δ_e, was then calculated as F_e/k = 191.7 mm. The total strength, F_{y2}, of all oscillators obtained considering a lateral force reduction factor, R, of 4. That is, $F_{y2} = F_e/R$ = 47,920 N.

For the different analyses:

a) The lower yield strength, F_{y1}, is obtained as βF_{y2} according to Equation 1, where β is varied.
b) The gap, Δ_{gap}, was defined as $\alpha\Delta_e$ where α is varied. This relationship is given in Equation 2. This gap is provided in both directions, so the total distance between the peak sliding in one direction, and that in the opposite direction is therefore $2\Delta_{gap}$.

$$\alpha = \Delta_{gap}/\Delta_e \quad (2)$$

To evaluate the sensitivity of peak and residual oscillator displacements were evaluated with gap ratios, α, equal to 0.2, 0.4, 0.6, 0.8, and strength ratios, β, equal to 0.25, 0.5, 0.75 so that the gap and strength values corresponding to the minimum response could be obtained. Furthermore an additional analysis was conducted corresponding to an elastoplastic loop. This is equivalent to using $\beta = F_{y1}/F_{y2} = 1.0$ and/or $\alpha = \Delta_{gap}/\Delta_e = 0$.

A transient analysis type was used with a Modified Newton algorithm. The integration timestep of 0.005 s was used and found to be sufficiently small to not cause significant differences in the response. An initial stiffness proportional Rayleigh model, with 5% damping at periods of 1.0s and 0.047s, was used. Analyses were run in batch mode.

3 BEHAVIOUR

The push-pull response in Figure 4 validates the response when the displacement applied is +/-12mm and the strength ratio, $\beta = F_{y1}/F_{y2}$, is 0.5. It may be seen that the gap value, Δ_{gap}, is the sliding distance in each direction. When Δ_{gap} is 0mm, the behaviour is elastoplastic with the structure reaching the strength F_{y2}, and there is no multistage effect. When the gap is 15mm, and the second stage is not reached, so the response is again elastoplastic with the lower strength F_{y1}. When Δ_{gap} is 6mm, the first and second stages are apparent and this loop has dynamic stability. The behaviour with a net negative post-elastic stiffness, giving some indication of a possible P-delta effect, is given in Figure 4b. The slightly different strength is due to the modelling of the 2 elements in Figure 3, This behaviour is different from the expected P-delta effect which would simply rotate the curve, but it may be considered as a reasonable approximation to it.

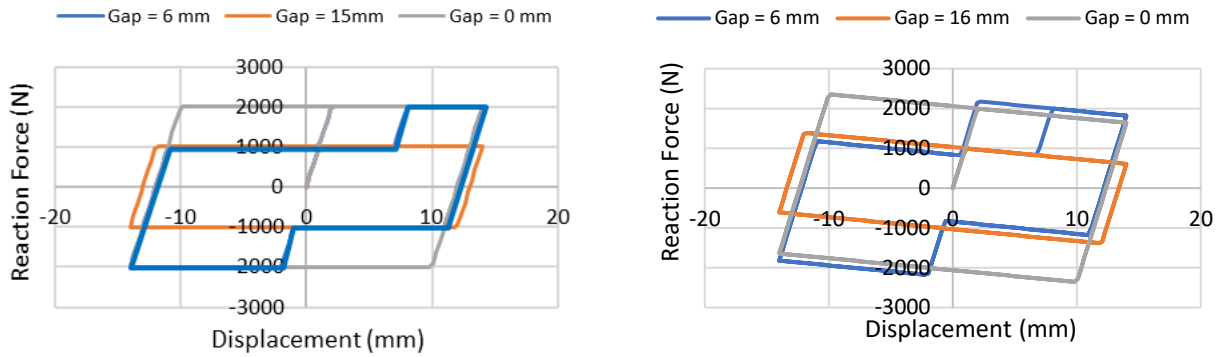

(a) Zero Post-Elastic Stiffness *(b) Negative Post-Elastic Stiffness*

Figure 4. *Push-Pull Behaviour* (β = 0.5).

For time history analysis, when there is no gap (i.e. α = 0), the peak displacement were 239mm and 326mm with zero and negative post elastic stiffness respectively as shown in

Zero Post-Elastic Stiffness (b) Negative Post-Elastic Stiffness

Figure . It may be seen that structures with all strength ratios had the same response when the gap ratio was zero as would be expected because the structure is elastoplastic.

As gap ratio, α, increased, the peak displacements tended to decrease and then increase because the dynamic stability, represented by the hysteresis centre curve (HCC) is more positive over the range considered initially. Then, when the gap ratio, α, is too big, the behaviour also tends toward elastoplastic with a lower strength, so the peak displacement increases. The tendency for reduced displacement was most significant for strength ratios, β, greater than 0.25. That is, for very low β the structure has initial slip, and low effective period compared to larger β.

For the zero post-elastic stiffness case, the displacement reduced to 94% of the elastoplastic value and it was less than 0.96 of the elastoplastic value (i.e. 3% greater than the minimum) over the range of about α = 0.15 to 0.45 when β = 0.5 and 0.75. This is not significant compared to the negative post-elastic stiffness case where ratcheting occurred. Here, the displacement decreased to 231/326 = 71% of the elastoplastic value. It was no more than 60% greater than this over the range of about α = 0.30 to 0.7.

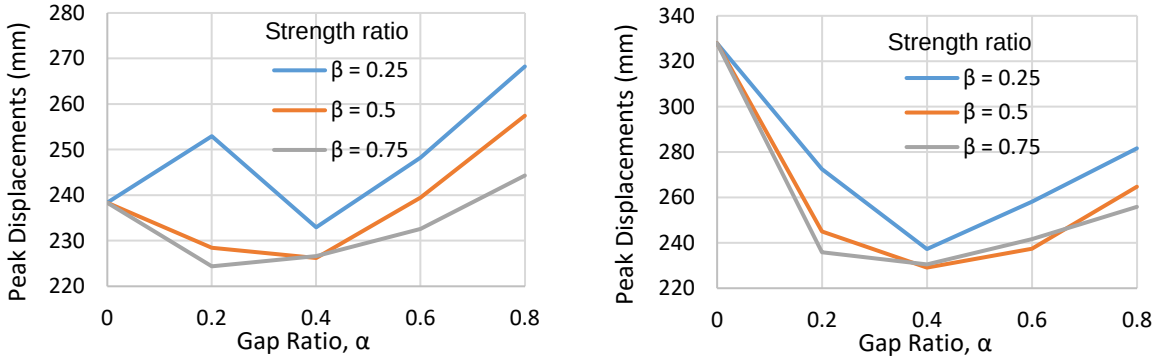

(a) Zero Post-Elastic Stiffness *(b) Negative Post-Elastic Stiffness*

Figure 5. *Peak displacements from Time History Analysis*

For time history analysis, when there is no gap (i.e. α = 0), the residual displacements were 76mm and 240mm with zero and negative post-elastic stiffness respectively as shown in

Zero Post-Elastic Stiffness (b) Negative Post-Elastic Stiffness

Figure . This shows the significant of seismic ratcheting when the post-elastic stiffness is negative. Again, structures with all strength ratios had the same response when the gap ratio was zero because the structure is elastoplastic.

As gap ratio, α, increased, the peak displacements tended to decrease and then increase for the same reasons as for peak displacements. There seemed to be some scatter with β, but no strong trends.

For the zero post-elastic stiffness case, the displacement reduced to 78% of the elastoplastic value and it was less 20% greater than this minimum over the range of about α = 0.35 to 0.7 when β = 0.5 and 0.75. This is not significant compared to the negative post-elastic stiffness case where the displacement decreased to as low as 62/240 = 26% of the elastoplastic value. It was no more than 20% greater than this minimum over the range of about α = 0.30 to 0.55 when β = 0.5 and 0.75.

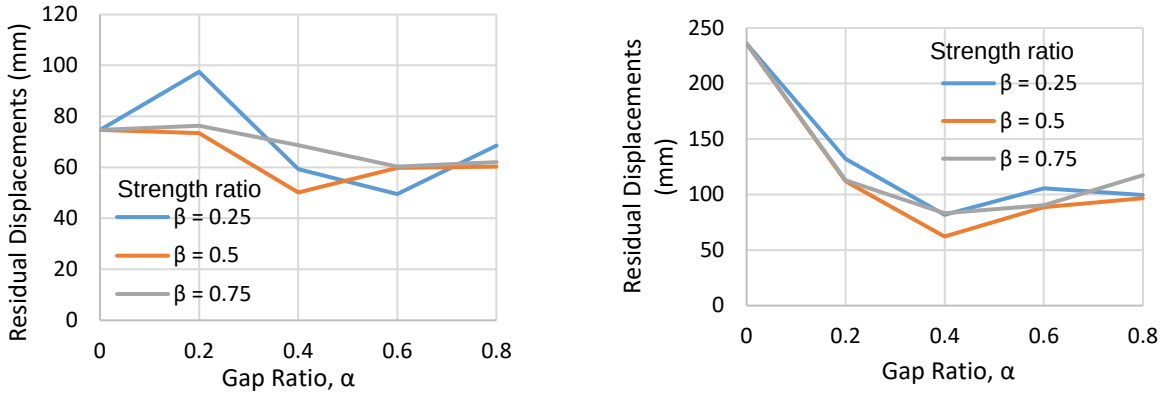

(a) Zero Post-Elastic Stiffness *(b) Negative Post-Elastic Stiffness*

Figure 6. *Residual displacements from Time History Analysis*

From the above it may be seen that the MFC could be beneficial for the zero post-elastic stiffness case even though there was not a lot of ratcheting. However, the effect is not large because the equal displacement assumptions still seem to hold, with not much change in peak response for this structure. However, the MFC was always strongly beneficial for the structure with negative post-elastic stiffness in terms of peak and residual displacements. A strength ratio, β, in the approximate range of 0.50-0.75, and a strength ratio, α, in the approximate range of 0.20-0.60, seemed to give lowest peak and residual displacements.

4 CONCLUSIONS

This paper describes the construction and seismic behaviour of simple structures with multi-stage friction connections (MFCs). In particular, it was shown that:

1) Multistage friction connections (MFCs) have a simple deformation mechanism which permits sliding on one surface and then later on the another surface. This produces a structural hysteresis loop with multiple strength ‘stages’. The relative strengths of the stages can be controlled by changing the relative number,

2) A simple numerical model was developed which enabled the characteristics of the MFC to be represented. The shape developed represented the behaviour seen from experimental tests well.

3) For a simple single mass structure, with a period of 1s, and a lateral force reduction factor of 4.0, subject to a suite of earthquake records, it was shown that the MFC reduced peak and residual displacements by up to 29% and 74% respectively. The response reduction was much more significant on the structure with a negative post-elastic stiffness. The displacements were lowest when the MFC gap ratio was in the range of about 0.50-0.75, and a strength ratio was in the approximate range of 0.20-0.60, for the structures

considered. The use of such a simple and economical device may be beneficial especially in structures which would otherwise be prone to ratcheting.

4. ACKNOWLEDGMENTS

This work described here was based on the undergraduate research project by Brosnan and El-Mashalgi (2023). Support and supervision were provided by MacRae, Luo, and Chanchi Golondrino.

4. REFERENCES

Baloch M. H., MacRae G. A. & Lee C-L. “Seismic ratcheting considerations”, NZSEE 2024 Conference. Paper 0009.

Brosnan R. C. A. and El-Mashalgi B. A. A., Multistage Friction Connection Optimisaton, Undergraduate Research Paper 2023, University of Canterbury, Christchurch, New Zealand. With support provided by MacRae, Luo and Chanchi.

Hariri, B., and Tremblay, R. (2019). “Stability of BRB frames under long duration subduction earthquakes.” 12th Canadian Conference on Earthquake Engineering.

Chanchi, J. C., Coral, H. A., and MacRae, G. A. (2023). "Multistage Friction Connections." NZSEE 2023 Conference. Paper 35.

Chanchí Golondrino, J. C., MacRae, G. A., Chase, J. G., Rodgers, G. W., Clifton, G. C. 2020. Seismic Behaviour of Symmetric Friction Connections for Steel Buildings, *Engineering Structures*, Vol 224, DOI: *https://doi.org/10.1016/j.engstruct.2020.111200*

Chanchí Golondrino J. C., Riascos Montenegro D. A., and MacRae G. A., Seismic Symmetric Friction Dissipater for Steel Braced Frames, Steel Structures in Seismic Areas (STESSA Conference), Salerno, July 2024.

MacRae, G. A. 2021. Multistage Friction Connections – Idea Proposal, *Hera Innovation in Metals*.

Christopoulos C., Tremblay, R., Kim H.-J., and Lacerte M., 2008. Self-Centering Energy Dissipative Bracing System for the Seismic Resistance of Structures: Development and Validation, Journal of Structural Engineering, 134(1), https://doi.org/10.1061/(ASCE)0733-9445(2008)134:1(9).

Dehghanian S., MacRae G. A., Moghadam A. S. “P-delta or P-theta analysis?”, NZSEE 2024 Conference. Paper 0149.

Fiorino L., Shakeel, S., Macillo, V., and Landolfo, R. (2017). "Behaviour factor (q) evaluation the CFS braced structures according to FEMA P695." Journal of Constructional Steel Research.

Khoo H. H., Clifton G. C., Butterworth J., MacRae G. A., Gledhill S. and Sidwell G., 2012. “Development of the Self-Centring Sliding Hinge Joint with Friction Ring Springs”, Journal of Constructional Steel Research, 78 (2012), 201–211.

Li G. Q, Jin H-J., Pang M-D., Sun Y-Z., Hu D-Z., and Sun F-F., 2022, Development and Application of Multi-stage Steel Dampers”, Proceedings of the 10th International Conference on Behaviour of Steel Structures in Seismic Areas, January. DOI: 10.1007/978-3-031-03811-2_5.

MacRae, G. A., and Kawashima, K. (1991). "Effect of Post-Elastic Stiffness on the Seismic Response of Single Degree of Freedom Structures." Proceedings, Japan Society of Civil Engineering Symposium on Earthquake Engineering, Tokyo.

MacRae G. A. and Kawashima K. (1993). "The Seismic Response of Bilinear Oscillators Using Japanese Earthquake Records", Journal of Research of the Public Works Research Institute, Vol. 30, Ministry of Construction, Japan.

MacRae, G. A. (1994). "P-delta Effects on Single-Degree-of-Freedom Structures in Earthquakes." Earthquake Spectra, 10(3), 539-568.

MacRae, G. A., and Kawashima, K. (1997). "Post-Earthquake Residual Displacements of Bilinear Oscillators." Earthquake Engineering and Structural Dynamics, 26, 701-716. https://doi-org.ezproxy.canterbury.ac.nz/10.1002/(SICI)1096-9845(199707)26:7<701::AID-EQE671>3.0.CO;2-I

MacRae G. A. and Kawashima K. (2001). "Seismic Behavior of Hollow Stiffened Steel Bridge Columns", ASCE Journal of Bridge Engineering, 6(2), Mar/Apr, pp 110-119.

MacRae G. A., Kimura Y., & Roeder C. W. (2004). "Effect of Column Stiffness on Braced Frame Seismic Behaviour", Journal of Structural Eng., ASCE. Journal of Structural Engineering, March, 130(3), pp.381-391.

MacRae G. A. (2011). "The Continuous Column Concept – Development and Use", Proceedings of the Ninth Pacific Conference on Earthquake Eng. (PCEE), Building an Earthquake-Resilient Society, 14-16 April.

MacRae G. A., Lee, C. L., and Yeow, T. Z. (2023a). "Considerations for Seismic Ratcheting." NZSEE 2023 Conference, 136-143.

MacRae, G. A. (2021). "Multistage Friction Connections", Idea Register, *NZ Heavy Engineering Research Association*.

MacRae G. A., (2023). The Christchurch Rebuild and Frictional Energy Dissipation for Structures in Seismic Regions, 13th Pacific Structural Steel Conference (PSSC) 2022, Century City International Convention Centre, 198, Century City Boulevard, Chengdu, 610041, Chengdu, China, 27-30 October.

MacRae G. A., Jia L-J., Yan Z., Clifton G. C., Ramhormozian S., Dhakal R., Xiang P., Rodgers G., Zhao X., (2023b). "ROBUST Test Programme Developments", The Tenth Kwang-Hua (光华) Forum on Innovations & Implementations in Earthquake Engineering Research, Tongji Architectural Design (Group) Co., Ltd. (TJAD), No.1230 Siping Road, Yangpu District, Shanghai, China, 8-11 December.

Robertson J. B. Edwards W. S., Luo Z., MacRae G. A., "Seismic response of frames with building cladding elements", NZSEE 2024 Conference. Paper 0139.

Saif, K. Z., Yeow, T. Z., Lee, C. L., MacRae, G. A. (2022). "Interpretation and Evaluation of NZS1170.5 2016 Provisions for Seismic Ratcheting." Bulletin of the NZSEE, 55(3), 183-198.

Sitler, B., Takeuchi, T., Matsui, R., Terashima, M., Terazawa, Y. (2020). "Experimental Investigation of a Multistage Buckling-Restrained Brace." Engineering Structures, 222.

Sitler B. and Takeuchi T., (2021). Reducing residual drift with multistage buckling restrained braces, 2020/2021 WCEE, Paper 2g 0022.

NZS1170.5 (2004). "NZS1170.5:2004, Earthquake Actions", Standards New Zealand.

Tremblay R. and Darwiche K. (2023). "A New Braced-Frame System for Self-Centering and Damage-Free Seismic Response for Low-Rise Steel Building Structures", Canadian Conference - Pacific Conference on Earthquake Engineering 2023, Vancouver, British Columbia, June 25th – June 30th.